

602664

2 of 3

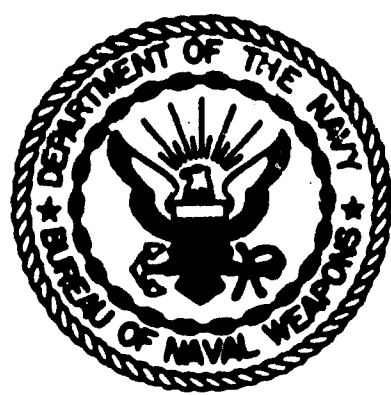
NWL Report No. 1919

A HEAT TRANSFER MODEL STUDY  
OF THE HOT WIRE INITIATOR

by

J. M. Massey, Jr.  
Warhead and Terminal Ballistics Laboratory

43 p  
hc ~ 2.00  
mf ~ 0.50



DDC  
R  
JUL 24 1964  
R  
DDC-IRA B

U. S. NAVAL WEAPONS LABORATORY  
DAHLGREN, VIRGINIA

U. S. Naval Weapons Laboratory  
Dahlgren, Virginia

A Heat Transfer Model Study  
of the Hot Wire Initiator

by

J. M. Massey, Jr.  
Warhead and Terminal Ballistics Laboratory

NWL Report No. 1919

WEPTASK NOS. RMMO-33-020/210-1/F008-11-01  
and RMMO-33-020/210-1/F008-17-01

6 July 1964

CONTENTS

	<u>Page</u>
Abstract. . . . .	iii
Foreword. . . . .	iv
Introduction. . . . .	1
Mathematical Model. . . . .	1
I. Equation of Conduction of Heat . . . . .	1
II. Simplifying Assumptions. . . . .	2
III. Final Equations. . . . .	3
Results . . . . .	9
Concluding Remarks. . . . .	12
References. . . . .	13
Appendices:	
A. Approximation of First and Second Partial Derivatives and the Laplacian by Finite Differences - Unequal Segments and Cylindrical Coordinates	
B. Distribution	

-----

Figures:

1. Cross Section of a Hot Wire Initiator (MARK 45 MOD 0 Cartridge)
2. Detail of MARK 45 MOD 0 Bridgewire and Bead with Coordinate System Superimposed
3. Spatial Distribution of Temperature Stations in Bridgewire and Bead
4. Interpolation Construction for  $\theta_{n,s}$
5. Sensitivity of MARK 45 MOD 0 Impulse Cartridge to Constant DC Current
6. Determination of Heat Transfer Film Coefficient and Thermal Conductivity
7. Bead Temperature ( $\theta_{c,s}$ ) vs Time
8. Steady State Radial Temperature Distribution -  $I=3$  amps
9. Steady State Axial Temperature Distribution -  $I=3$  amps
10. Effect on Sensitivity of a 20% Increase in  $T_a$
11. Effect on Sensitivity of a 20% Increase in  $h$

CONTENTS (Continued)

## Figures (Continued):

12. Effect on Sensitivity of a 20% Increase in  $k$
13. Effect on Sensitivity of a 20% Decrease in  $\rho c$
14. Effect on Sensitivity of a 50% Increase in  $r_{\text{bead}}$
15. Effect on Sensitivity of a 50% Increase in  $L$
16. Finite Difference Construction for  $\frac{\partial^2 \theta}{\partial r^2}$ ,  $\frac{\partial \theta}{\partial r}$ ,  $\frac{\partial^2 \theta}{\partial x^2}$  and  $\nabla^2 \theta$

## Table:

1. Input Parameters and Material Composition

ABSTRACT

A mathematical heat transfer model, applicable to determining the sensitivity to input current of a hot wire initiator, is developed. Simplifying assumptions are introduced which make the model amenable to solution using a medium size analog computer. The model is applied to the MARK 45 MOD 0 impulse cartridge. Solutions are compared to empirical sensitivity data for this cartridge conditioned at  $-80^{\circ}\text{F}$ ,  $68^{\circ}\text{F}$  and  $225^{\circ}\text{F}$ .

FOREWORD

The development of the mathematical model, computations, and experimental work summarized in this report was carried out under Problem Assignment 1 of WEPTASKS NOS. RMMO-33-020/210-1/F008-11-01 and RMMO-33-020/210-1/F008-17-01.

The author is indebted to Mr. George L. Poudrier for his extensive suggestions and comments which proved beneficial to developing the mathematical model presented here and for his assistance in judiciously choosing the simplifying assumptions. Additionally, Mr. Poudrier assisted materially in the operation of the analog computer. The author's appreciation is extended to Mr. R. L. Montgomery for his time spent both in checking the analog computer program and in assisting in the operation of the computer. Finally, the author is indebted to Mr. S. E. Hedden, who suggested the problem and the approach to its solution.

This report has been reviewed by the following personnel of the Warhead and Terminal Ballistics Laboratory:

- S. E. HEDDEN, Head, Research Branch, Cartridge  
Actuated Devices Division
- J. J. GLANCY, Head, Cartridge Actuated  
Devices Division
- W. E. MCKENZIE, Assistant Director for Technical  
Applications, Warhead and Terminal  
Ballistics Laboratory
- R. I. ROSSBACHER, Director, Warhead and Terminal  
Ballistics Laboratory

APPROVED FOR RELEASE:

/s/ RALPH A. NIEMANN  
Acting  
Technical Director

## INTRODUCTION

A hot wire initiator (see Figure 1) is a single discrete unit containing an explosive, propellant, or pyrotechnic material commonly referred to as the primary mix or bead material; hereafter referred to as the bead. The bead usually surrounds a fine wire known as the bridgewire which spans or bridges two pins as shown in Figure 1. The bead is ignited by ohmic heating of the bridgewire when sufficient electric potential is applied across the pins. The ignited bead in turn ignites a secondary charge known as the booster or main charge, as the case may be.

Of interest to the designer of a hot wire initiator is the control of its sensitivity. Here sensitivity refers to the relation between the firing time of an initiator and the input firing stimulus such as current or potential. The problem of determining the sensitivity of a newly designed hot wire initiator was treated, in the study reported here, as a heat transfer phenomenon. A mathematical model was developed whose solutions yield the sensitivities of hot wire initiators. The model was then applied to the MARK 45 MOD 0 Impulse Cartridge. In order to obtain values for two inaccurately known parameters (the thermal conductivity of the bead and the heat transfer film coefficient of the bridgewire-bead interface), they were systematically varied until, through trial and error, the calculated sensitivity matched the measured sensitivity at two values of input current. In this way the model was calibrated against empirical firing time versus firing current data from cartridges conditioned at room temperature. The degree of fit between the calculated and empirical data for other values of input current and at different conditioning temperatures was used as a measure of the adequacy of the model.

Finally, certain of the inaccurately known parameters were arbitrarily changed, one at a time, to determine the sensitivity of the solutions to possible error in the parameter changed.

All solutions were obtained on an Electronic Associates analog computer consisting of an eighty amplifier TR-10 four cabinet complex.

## MATHEMATICAL MODEL

### 1. Equation of Conduction of Heat -

Reference (a), page 10, gives the heat conduction equation for an isotropic, homogeneous solid with internal heat generation as

$$\frac{\partial \theta}{\partial t} = a \nabla^2 \theta + \frac{A(x, y, z, t)}{k}, \quad (1)$$

where:

$a = \frac{k}{\rho c}$  is the thermal diffusivity,

$A$  is the rate of heat produced per unit time per unit volume at the point  $(x,y,z)$ ,

$c$  is the specific heat,

$k$  is the thermal conductivity,

$\rho$  is the density,

$\theta$  is the instantaneous temperature at the point  $x,y,z$ ,

$\nabla^2$  is the Laplacian operator.

## II. Simplifying Assumptions -

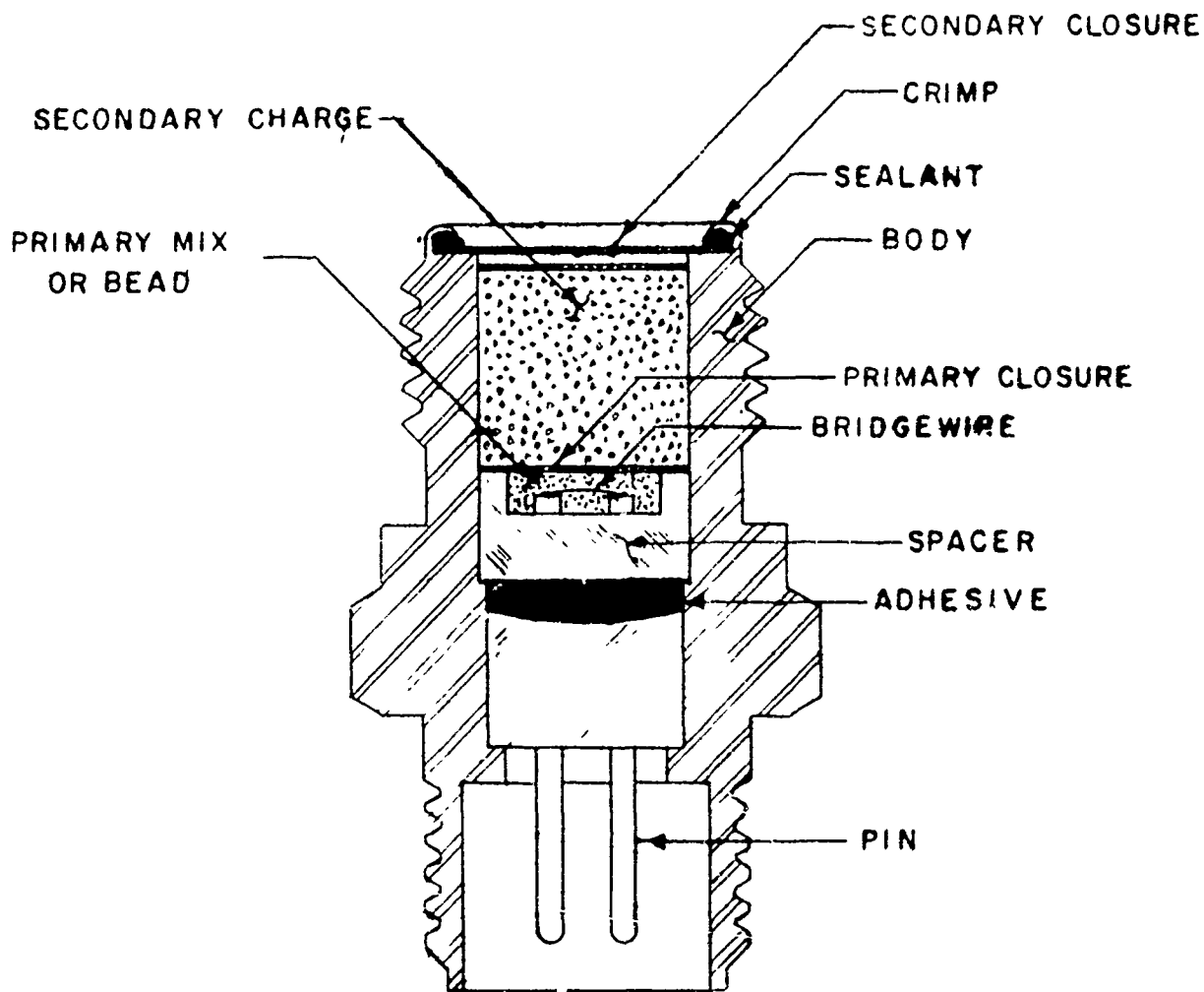
In order to obtain a mathematical model within reach of the capabilities of the computing equipment used, the following simplifying assumptions were made:

A. Radial temperature distributions in the bridgewire were neglected. From equation (1), page 204 of reference (a), it was concluded that the difference between the outer surface temperature and the center temperature of the bridgewire of the MARK 45 MOD 0 cartridge (the hot wire initiator used in this analysis) would never exceed  $1.34^\circ\text{C}$ . This difference was considered negligible since it is only 0.5% of the assumed autoignition temperature of the bead.

B. Although the MARK 45 MOD 0 cartridge is a four pin double bridge hot wire initiator, only one of the bridge circuits was considered in the study. Figure 2 is a sketch, with coordinate system superimposed, of the bridgewire and bead of the MARK 45 MOD 0 cartridge. Only one of the bridgewires is shown. The other bridgewire is parallel to the one shown and is electrically insulated from it.

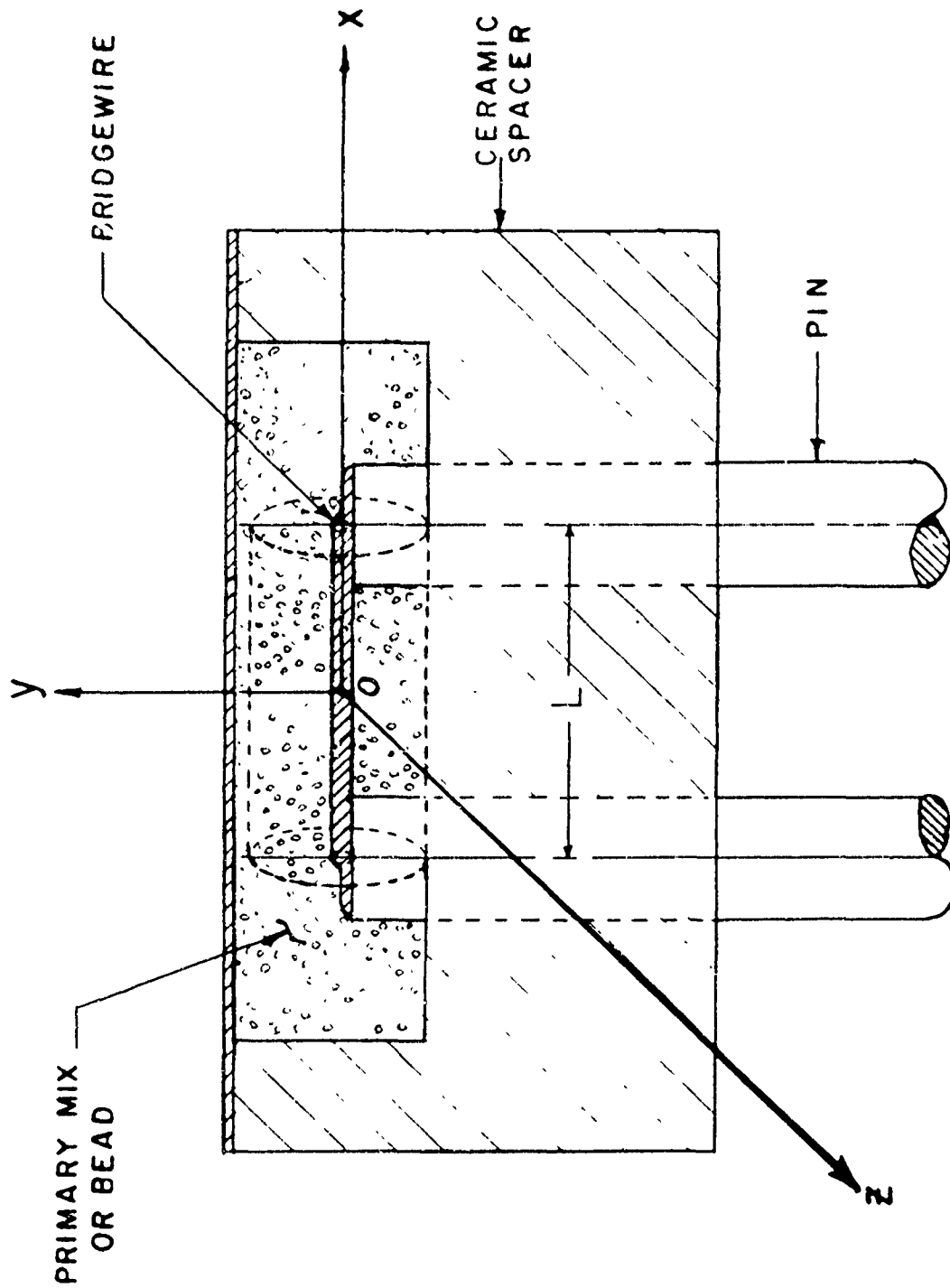
C. Cylindrical symmetry was assumed.

D. As depicted by the broken lines in Figure 2, an arbitrary cylindrical boundary was introduced. In the mathematical model this was assumed to be the outer boundary of the bead and was assumed to remain at ambient temperature. This assumption was based on the concept that the temperature of the relatively large masses of the pins and the ceramic plug probably does not differ appreciably from ambient.



SCALE: 4/1

FIGURE 1  
 CROSS SECTION OF A HOT WIRE INITIATOR  
 (MARK 45 MOD 0 CARTRIDGE)



SCALE: 20/1

FIGURE 2

DETAIL OF MARK 45 MFD O BRIDGE WIRE AND LEAD WITH COORDINATE SYSTEM SUPERIMPOSED

E. The thermal properties (e.g., thermal conductivity, specific heat, and diffusivity) of the initiator materials were assumed to be independent of temperature. Approximately median values for these properties were chosen consistent with the temperature range encountered.

F. The exothermic chemical self heating of the bead was assumed negligible until the bead reached a critical temperature  $T_a$ . Ignition was assumed to occur at this time and all subsequent calculations were disregarded. The value chosen for  $T_a$  was based on experimental evidence of an exothermic reaction in the bead when the initiator was subjected to various oven temperatures. In accord with the experimental technique for determining the value of  $T_a$ , it is referred to as the autoignition temperature.

### III. Final Equations -

Let primed symbols refer to the bridgewire and let unprimed symbols refer to the bead. Also let  $\theta$  ( $\theta'$ ) now refer to the temperature difference between the bead (bridgewire) and ambient. As developed in sections 4.2 and 4.10 of reference (a), equation (1) applied to the bridgewire becomes

$$\frac{\partial \theta'}{\partial t} = a' \nabla^2 \theta' + \frac{I^2 J (1 + \alpha' \theta')}{\rho' (A')^2 c' \sigma'} - \frac{P' h}{\rho' A' c'} (\theta' - \theta_s), \quad (2)$$

where:

$A'$  is the cross sectional area of the bridgewire,

$a'$  is the diffusivity of the bridgewire,

$h$  is the heat transfer film coefficient of the bridgewire-bead interface,

$I$  is the instantaneous current in the wire,

$J$  is the mechanical equivalent of heat,

$t$  is the time,

$\alpha'$  is the temperature coefficient of resistivity,

$\theta_s$  is the surface temperature of the bead at the bridgewire-bead interface.

Equation (1) applied to the bead simplifies to

$$\frac{\partial \theta}{\partial t} = a \nabla^2 \theta, \quad (3)$$

where  $a$  is the diffusivity of the bead.

The initial, boundary, and terminal conditions are

$$\theta = \theta' = 0 \text{ at } t = 0, \quad (4)$$

$$\theta = \theta' = 0 \text{ at } x = \pm \frac{L}{2}, \quad r = r_{\text{bead}}, \quad (5)$$

$$\theta'(-x) = \theta'(x), \quad (6)$$

$$\theta(-x) = \theta(x), \quad (7)$$

$$-k \frac{\partial \theta}{\partial r} = h(\theta' - \theta_s) \text{ at } r = r_s, \quad (8)$$

$$\theta < T_a - T_c, \quad (9)$$

where,

$L$  is the length of the bridgewire and the bead,

$r_{\text{bead}}$  is the outer radius of the bead,

$r_s$  is the inner radius of the bead (equal to the bridge-wire radius),

$T_c$  is the ambient temperature.

Equations (2) and (3) can be approximated by a set of ordinary differential equations with time as the independent variable. This is done by considering  $\theta'$  at discrete values of  $x$  and by considering  $\theta$  at discrete values of  $x$  and  $r$ . The partial derivatives of  $\theta'$  with respect to  $x$  and of  $\theta$  with respect to  $x$  and  $r$  are then represented by appropriate difference expressions (see Appendix A).

Two independent investigations were made to determine the distribution and the minimum number of discrete values of  $x$  and  $r$  at which the temperatures must be computed to obtain reasonable accuracy.

Computational experiments involving up to 6 axial temperature stations in half the bridgewire length (equivalent to 12 axial stations) showed that 3 equally spaced axial stations in half the bridgewire and bead length was sufficient. The error in computed temperatures introduced by using only 3 axial stations was about 3%. Similarly, computational experiments involving up to 6 radial temperature stations showed that 4 unequally spaced radial stations in the bead were sufficient. The error in computed temperatures introduced by using only 4 radial stations was less than 10%. This was provided the radial temperature station nearest the bridgewire-bead interface was chosen sufficiently close to the interface. It was determined that "sufficiently close" meant that the distance from the bridgewire-bead interface to the first radial temperature station should be less than 1% of the distance from the bridgewire-bead interface to the bead's outer radius.

In accordance with the conclusions reached, temperature stations were selected within the bridgewire and bead of the MARK 45 MOD 0 cartridge as indicated in Figure 3. Each station is assigned the generic indices  $n, m$  where  $n$  is the axial position index and  $m$  is the radial position index.  $n=0$  refers to any point in a plane perpendicular to the bridgewire and passing through its center.  $m=0$  refers to any point on the surface of a circular cylinder whose axis coincides with the axis of the bridgewire and whose radius is equal to the radial distance from the axis of the bridgewire to the row of stations within the bead nearest the bridgewire.

For the bridgewire

$$\nabla^2 \theta' = \frac{\partial^2 \theta'}{\partial x^2}. \quad (10)$$

From equation (A 13) in Appendix A, equation (10) can be approximated (with  $\beta=1$ ) by

$$\nabla^2 \theta' \Big|_{x=x_n} = \frac{1}{q^2} (\theta'_{n+1} - 2\theta'_n + \theta'_{n-1}). \quad (11)$$

Substituting from equation (11) into equation (2), combining terms, and imposing the initial, boundary, and symmetry conditions of equations (4), (5), (6) and (7), the final equations for the bridge-wire are

$$\left. \begin{aligned} \frac{d\theta'_n}{dt} &= \frac{I^2 J(1+\alpha'\theta'_n)}{\rho'(A')^2 c'\sigma'} + \frac{a'}{q^2} \theta'_{n+1} - \left( \frac{2a'}{q^2} + \frac{P'h}{\rho'A'C'} \right) \theta'_n \\ &+ \frac{a'}{q^2} \theta'_{n-1} + \frac{P'h}{\rho'A'C'} \theta'_{n,s} \\ n &= 0, 1, 2 \\ \theta'_{-1} &= \theta'_1 \\ \theta'_3 &= 0 \\ \theta'_n = \theta'_{n,s} &= 0 \text{ at } t=0. \end{aligned} \right\} (12)$$

In order to calculate  $\theta_{n,s}$ , a parabola lying in the  $r-\theta$  plane is fitted through the three points  $(-p_o, \theta_{n-1})$ ,  $(0, \theta_{n,o})$ , and  $(p_o, \theta_{n,1})$  as shown in Figure 4. The equation of this parabola with origin of the coordinate system arbitrarily chosen at radial station  $r=r_o$  is

$$\theta \Big|_{x=x_n} = A(r-r_o)^2 + B(r-r_o) + C. \quad (13)$$

or

$$\theta_{n,s} = A\left(-\frac{p_o}{2}\right)^2 + B\left(-\frac{p_o}{2}\right) + C. \quad (14)$$

The coefficients A, B, and C are derived in Appendix A. Substituting the values for A, B, and C from equations (A8), (A9), and (A10) into equation (14) results in the final expressions for the bead inner surface temperatures.

$$\left. \begin{aligned} \theta_{n,s} &= -\frac{1}{4\gamma(\gamma+1)} \theta_{n,1} + \frac{2\gamma+1}{4\gamma} \theta_{n,o} + \frac{2\gamma+1}{4(\gamma+1)} \theta_{n,-1} \\ n &= 0, 1, 2. \end{aligned} \right\} (15)$$



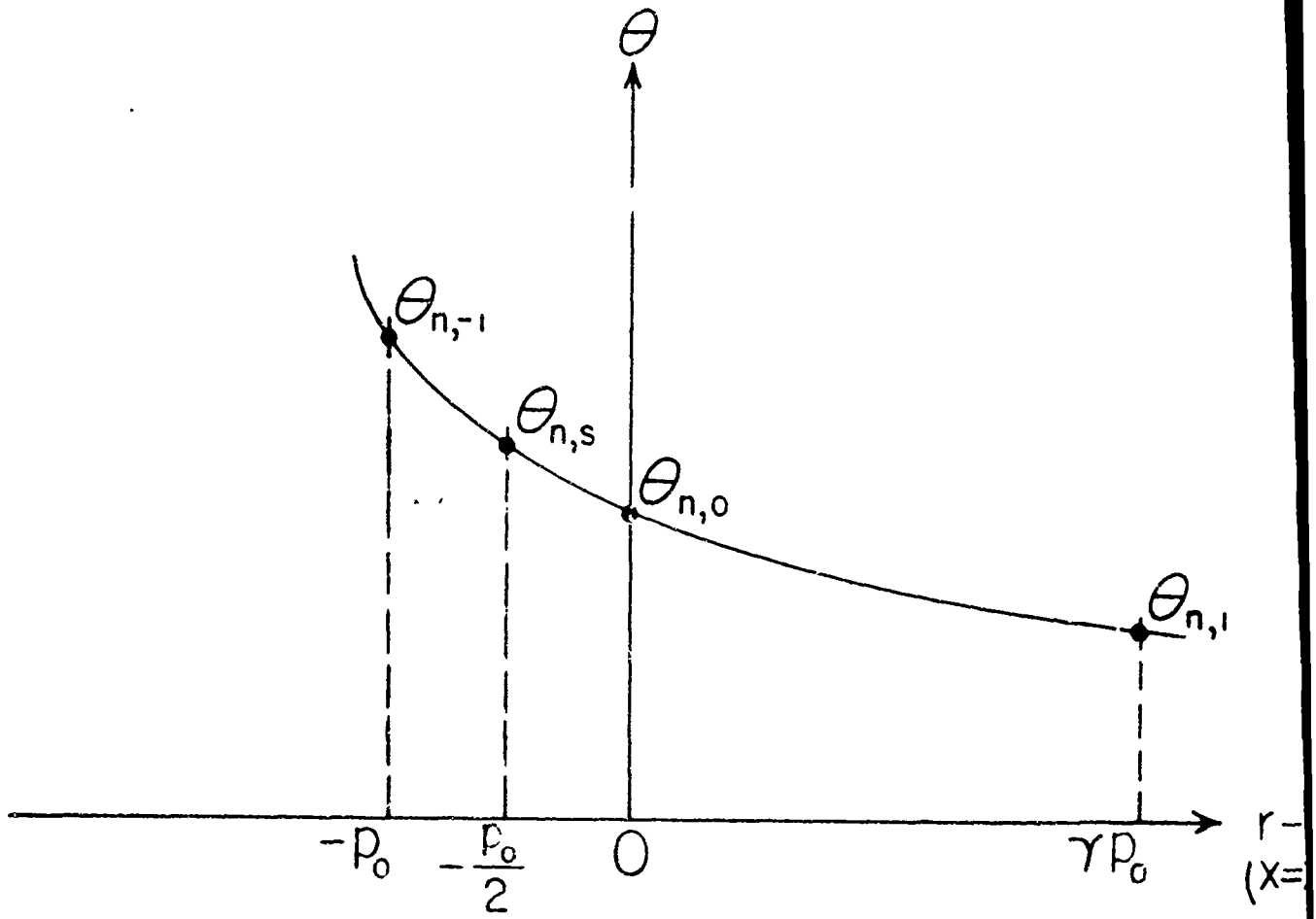


FIGURE 4

INTERPOLATION CONSTRUCTION FOR  $\theta_{n,s}$

The final form of the boundary condition, equation (8), can now be given. Substituting into equation (8) the finite difference approximation for  $\frac{\partial \theta}{\partial r}$ , derived in Appendix A (see equation (A11)), and the expressions for the bead surface temperature (equation (15)), and combining terms results in

$$\theta_{n,-1} = \left( \frac{\frac{h}{k}}{\frac{1}{p_o} + \frac{2\gamma+1}{4(\gamma+1)}} \right) \theta'_n + \left( \frac{\frac{1}{4\gamma(\gamma+1)} \frac{h}{k}}{\frac{h}{k} + \frac{2\gamma+1}{4(\gamma+1)} \frac{h}{k}} \right) \theta_{n,1} + \left( \frac{\frac{1}{p_o} - \frac{2\gamma+1}{4\gamma} \frac{h}{k}}{\frac{1}{p_o} + \frac{2\gamma+1}{4(\gamma+1)} \frac{h}{k}} \right) \theta_{n,c} \quad (16)$$

$$n = 0, 1, 2.$$

For the bead

$$\nabla^2 \theta = \frac{\partial^2 \theta}{\partial r^2} + \frac{1}{r} \frac{\partial \theta}{\partial r} + \frac{\partial^2 \theta}{\partial x^2}. \quad (17)$$

From equation (A14) in Appendix A, equation (17) can be approximated (with  $\beta=1$ ) by

$$\begin{aligned} \nabla^2 \theta \Big|_{\substack{x=x_n \\ r=r_m}} &= \left( \frac{2r_m + p_m}{\gamma(\gamma+1) p_m^2 r_m} \right) \theta_{n,m+1} \\ &- \left( \frac{2r_m + (1-\gamma) p_m}{\gamma p_m^2 r_m} + \frac{2}{q^2} \right) \theta_{n,m} \\ &+ \left( \frac{2r_m - \gamma p_m}{(1+\gamma) p_m^2} \right) \theta_{n,m-1} + \left( \frac{1}{q^2} \right) \theta_{n+1,m} \\ &+ \left( \frac{1}{q^2} \right) \theta_{n-1,m}. \end{aligned} \quad (18)$$

Substituting from equation (18) into equation (3) and imposing the initial, boundary, and symmetry conditions of equations (4), (5), (6), and (7); the final equations for the bead are

$$\begin{aligned}
 \frac{d\theta_{n,m}}{dt} = & \left( \frac{a(2r_m + p_m)}{\gamma(1+\gamma) p_m^2 r_m} \right) \theta_{n,m+1} \\
 & - \left( \frac{a(2r_m + (1-\gamma) p_m)}{\gamma p_m^2 r_m} + \frac{2a}{q^2} \right) \theta_{n,m} \\
 & + \left( \frac{a(2r_m - \gamma p_m)}{1+\gamma p_m^2 r_m} \right) \theta_{n,m-1} \\
 & + \left( \frac{a}{q^2} \right) \theta_{n+1,m} + \left( \frac{a}{q^2} \right) \theta_{n-1,m}
 \end{aligned} \tag{19}$$

$$\begin{aligned}
 \theta_{-1,m} &= \theta_{1,m} \\
 \theta_{n,4} &= 0 \\
 \theta_{3,m} &= 0 \\
 \theta_{n,m} &= 0 \text{ at } t=0 \\
 n &= 0,1,2. \\
 m &= 0,1,2,3.
 \end{aligned}$$

Equations (12), (15), (16), and (19) are the final equations for the bridgewire, bead inner surface temperature, boundary condition, and bead, respectively.

RESULTS

Empirical data of firing time versus constant DC current, for the MARK 45 MCD O cartridge at three conditioning temperatures, is presented in Figure 5. The vertical bars indicate the spread in the data. A smooth curve (not shown) was visually fitted to the room temperature data, and from this curve, the sensitivity at 4 and 10 amps was determined. Several values for the thermal conductivity  $k$  of the bead were chosen which were expected to bracket the true, but unknown, value. Using currents of 4 and 10 amps in the computer program, selected values of heat transfer film coefficients  $h$  for the bridgewire-bead interface were determined by trial and error. These values were selected such that the computed sensitivity matched the empirical sensitivity for each value of  $k$  chosen. By graphing the corresponding values of  $h$  vs  $k$  for 4 amps and for 10 amps respectively, it was determined that a single value of  $h$  and of  $k$  would satisfy the empirical sensitivity requirement at both 4 and 10 amps. This result is shown in Figure 6. This indirect method of measuring  $h$  and  $k$  is dependent on the adequacy of the mathematical model and the accuracy of the other parameters. Due to the large number of assumptions required in this study, no attempt was made to estimate the accuracy of the values obtained for  $h$  and  $k$ .

Table 1 lists the input parameters used in these and subsequent calculations. It also lists the composition of the initiator materials of interest here and the sources for information given.

TABLE 1                      INPUT PARAMETERS AND MATERIAL COMPOSITION

<u>Parameter</u>	<u>Symbol</u>	<u>Value</u>	<u>Source*</u>
Bridgewire:			
Length	$L, 6q$	0.2847 cm	1
Radius	$r_s$	$0.9010 \times 10^{-2}$ cm	1
Cross sectional area	$A'$	$2.554 \times 10^{-4}$ cm <sup>2</sup>	1
Perimeter	$P'$	$5.661 \times 10^{-2}$ cm	1
Electric conductivity	$\sigma'$	$1.00 \times 10^4$ mhos/cm	2
Thermal conductivity	$k'$	0.050 cal/sec-cm-°C	3
Density	$\rho'$	8.50 gm/cm <sup>3</sup>	4
Thermal capacity	$c'$	0.126 cal/gm-°C	4
Temperature coefficient of resistivity	$\alpha'$	$1.8 \times 10^{-4}$ (°C) <sup>-1</sup>	2

TABLE 1 (Continued)

<u>Parameter</u>	<u>Symbol</u>	<u>Value</u>	<u>Source*</u>
Bead:			
Length	L, $6q$	0.2847 cm	1
Inner radius	$r_s$	$0.9010 \times 10^{-2}$ cm	1
Outer radius	$r_{\text{bead}}, r_4$	$7.875 \times 10^{-2}$ cm	1
Thermal conductivity	k	$5.05 \times 10^{-4}$ cal/sec-cm- $^{\circ}$ C	5
Density	$\rho$	2.52 gm/cm <sup>3</sup>	4
Thermal capacity	c	0.2461 cal/gm- $^{\circ}$ C	4
Autoignition temperature	$T_a$	270 $^{\circ}$ C	6
Bridgewire-bead interface:			
Heat transfer film coefficient	h	0.116 cal/sec-cm <sup>2</sup> - $^{\circ}$ C	5
Bridgewire composition:			
Nickel	Ni	80%	1
Chromium	Cr	20%	1
Bead composition:			
Zirconium	Zr	7.00%	1
Ammonium dichromate	$(\text{NH}_4)_2\text{Cr}_2\text{O}_7$	14.08%	1
Ammonium perchlorate	$\text{NH}_4\text{ClO}_4$	44.92%	1
Barium chromate	$\text{BaCrO}_4$	34.00%	1

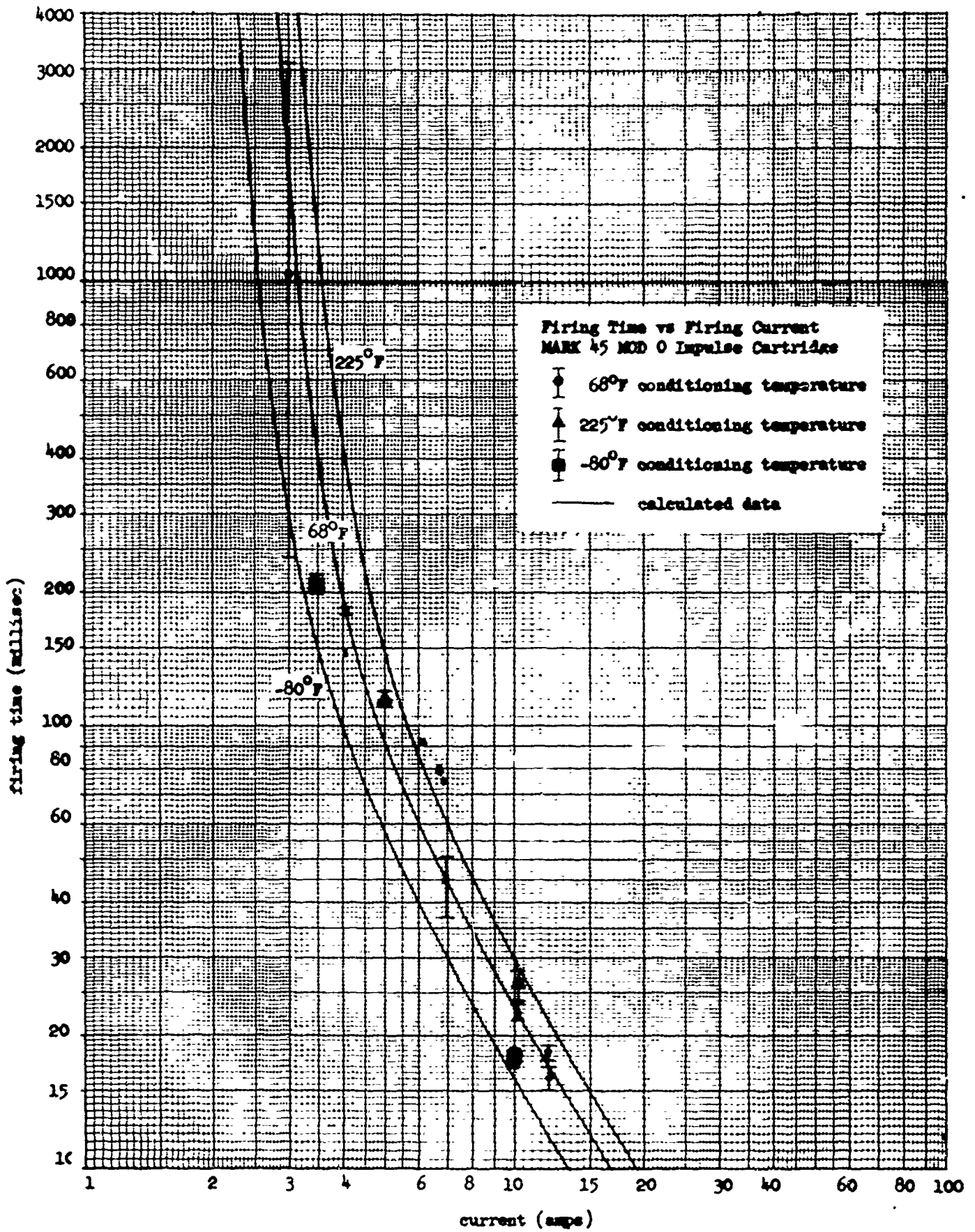


FIGURE 5

SENSITIVITY OF MARK 45 MOD 0 IMPULSE CARTRIDGE TO CONSTANT DC CURRENT

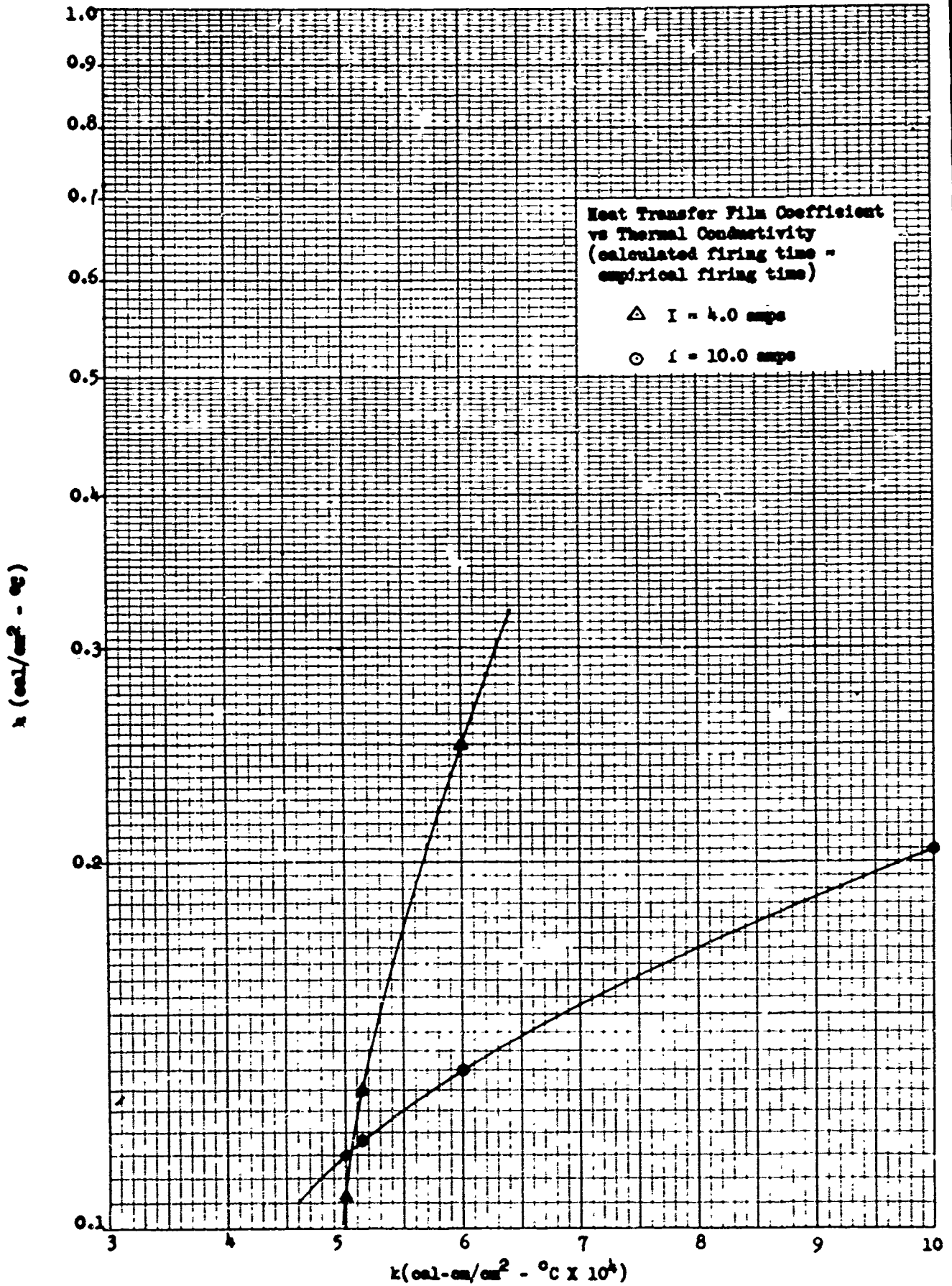


FIGURE 6

DETERMINATION OF HEAT TRANSFER FILM COEFFICIENT AND THERMAL CONDUCTIVITY

TABLE 1 (Continued)

## \*Source key

1. Either obtained directly or derived from information given in reference (d).
2. Obtained directly from reference (e).
3. Derived from information given in reference (f).
4. Derived from information given in reference (e). The derivation was based on values given for each component of the composition if it was available. If it was not available, the values for chemically similar compounds were used.
5. Derived by graphically fitting computed results to empirical data at two input currents.
6. Based on experimental evidence of an exothermic reaction in the bead when the initiator was subjected to various oven temperatures.

Using the values of  $k = 5.05 \times 10^{-4}$  cal/cm<sup>2</sup>-°C and  $h = 0.116$  cal/cm<sup>2</sup>-°C (the point of intersection in Figure 6), the bead temperature  $\theta_{o,s}$  of the MARK 45 MOD 0 cartridge was calculated for values of input current ranging from 3.0 to 20.0 amps. The  $\theta_{o,s}$  point was selected because it, being in the center and at the bead's inner surface (nearest the bridgewire), is always the hottest point in the bead. The initiator sensitivity for a given current and conditioning temperature, was then determined by observing the time required for  $\theta_{o,s}$  to reach a value equal to the difference between the assumed autoignition temperature of 270°C and the conditioning temperature. Conditioning temperatures of -80, 68, and 225°F were investigated. These correspond to -62.22, 20.00, and 107.2°C, respectively. The computed sensitivities at the three conditioning temperatures are presented by the three curves in Figure 5.

Figure 7 is a plot of  $\theta_{o,s}$  versus time for various currents. The intersections of these curves with the horizontal lines gives the times at which ignition is assumed to occur. The sensitivity curves of Figure 5 are derived from this information.

In Figure 7, the curve of  $\theta_{o,s}$  versus time, for  $I=3$  amps, indicates that a steady state temperature below the autoignition temperature would be reached at conditioning temperatures below -10°C (14.0°F). Hence, as an example, steady state temperatures

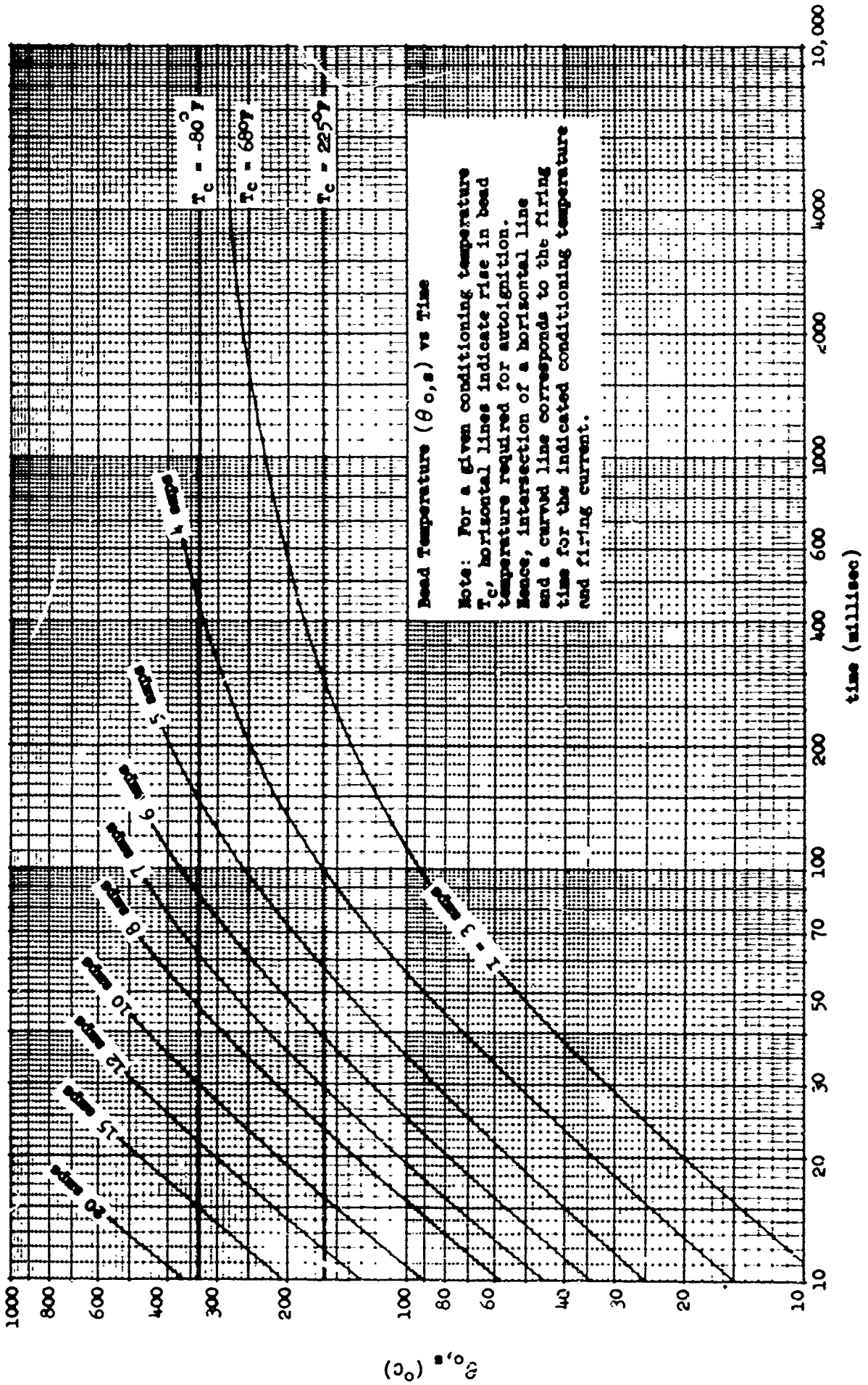
were computed for the bridgewire and bead for  $I=3$  amps. Figure 8 is a plot of these steady state temperatures versus radius  $r$ . Figure 9 is a plot of the same steady state temperatures versus axial position  $x$ .

Table 1 shows that values for  $h$ ,  $k$ ,  $\rho$ , and  $c$  (not being available in the literature) were estimated from related data. The geometry of the outer boundary was arbitrary and the autoignition temperature  $T_a$  was based on a gross experiment. To determine the sensitivity of the solutions to each of these parameters, the sensitivity of the MARK 45 MOD 0 cartridges was recalculated with each of the above parameters changed one at a time. Since  $\rho$  and  $c$  appear only as a product, only the product  $\rho c$  was changed. The input parameters  $T_a$ ,  $h$ , and  $k$  were each increased 20%. The product  $\rho c$  was decreased 20%. The bead radius and the bridgewire and bead length were each increased 50%. Each of these changes is reflected in the sensitivity of the initiator. In Figures 10 through 15, the new sensitivity is compared to that originally calculated and shown in Figure 5. The comparisons are made for a conditioning temperature of 68°F.

#### CONCLUDING REMARKS

A mathematical heat transfer model has been developed which is amenable to solution using a medium size analog computer. The model is applicable to determining the sensitivity of a conventional hot wire initiator. While the model has been applied only to the MARK 45 MOD 0 impulse cartridge, its ability to faithfully reproduce the room temperature sensitivity of this cartridge over a range of firing times from 15 to 1000 milliseconds demonstrates the adequacy of the model to account for the important parameters associated with a hot wire initiator of this basic design. Additionally, the model predicts with reasonable accuracy the sensitivity of the MARK 45 MOD 0 impulse cartridge conditioned at 225°F and at -80°F.

At present, fundamental data required as input to the model is only partially available. However, the usefulness of the model is not lost since, as was done in this study, the model can be calibrated to reproduce the available sensitivity data. The sensitivity for other conditions can then be predicted. For example, the model is not restricted to DC input currents. However, if the sensitivity to DC input currents is known then the model can be calibrated to reproduce this data. Subsequently, the model could serve as a powerful tool to predict the sensitivity to any time varying input current, e.g. sinusoidal. Or, it could be used to predict (or investigate) the effects on sensitivity of changing one or more design parameters such as the bridgewire material or bridgewire diameter.



**FIGURE 7**  
**BEAD TEMPERATURE ( $\theta_{0,s}$ ) VS TIME**

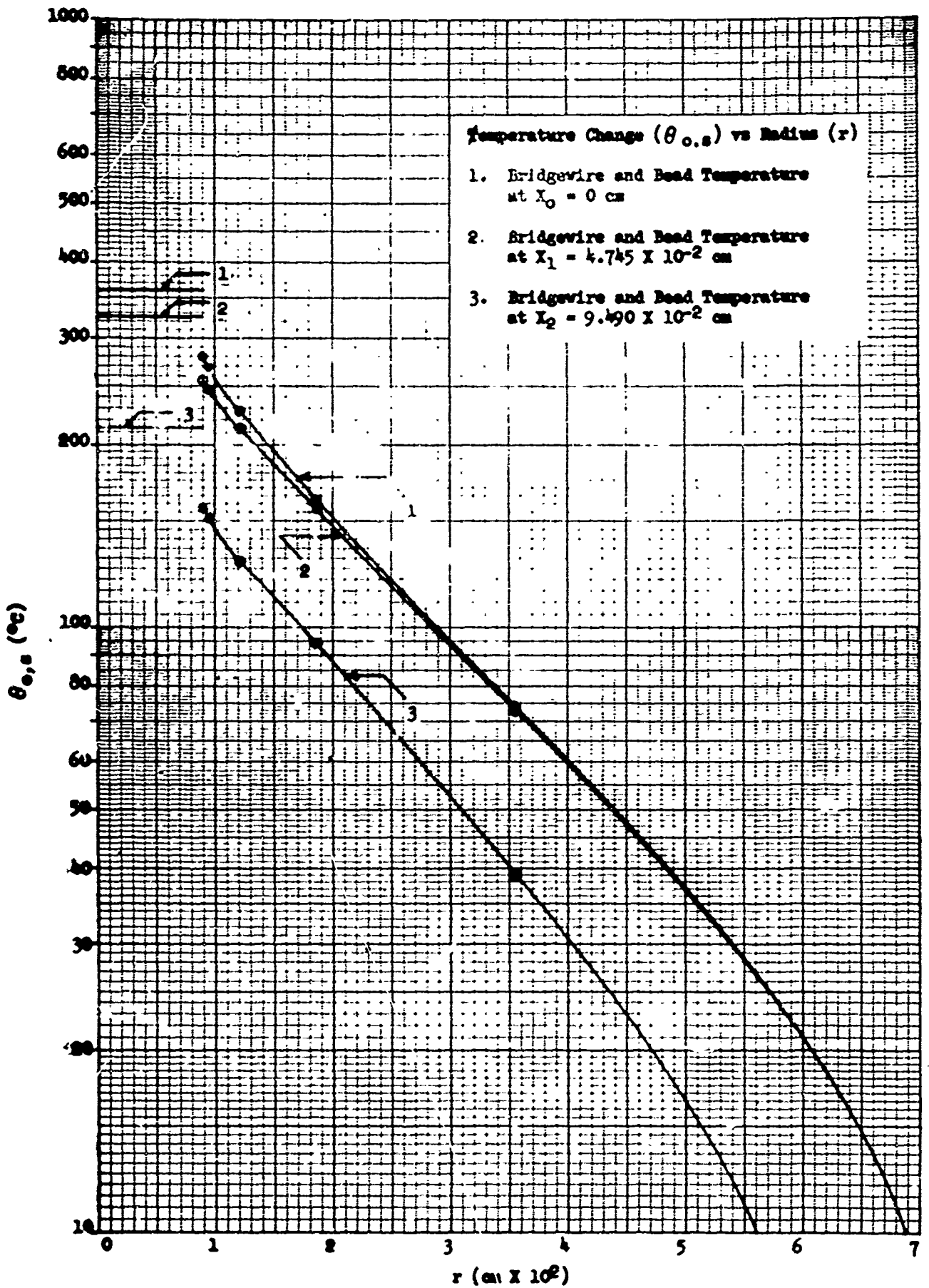


FIGURE 8

STEADY STATE RADIAL TEMPERATURE DISTRIBUTION - I = 3 AMPS

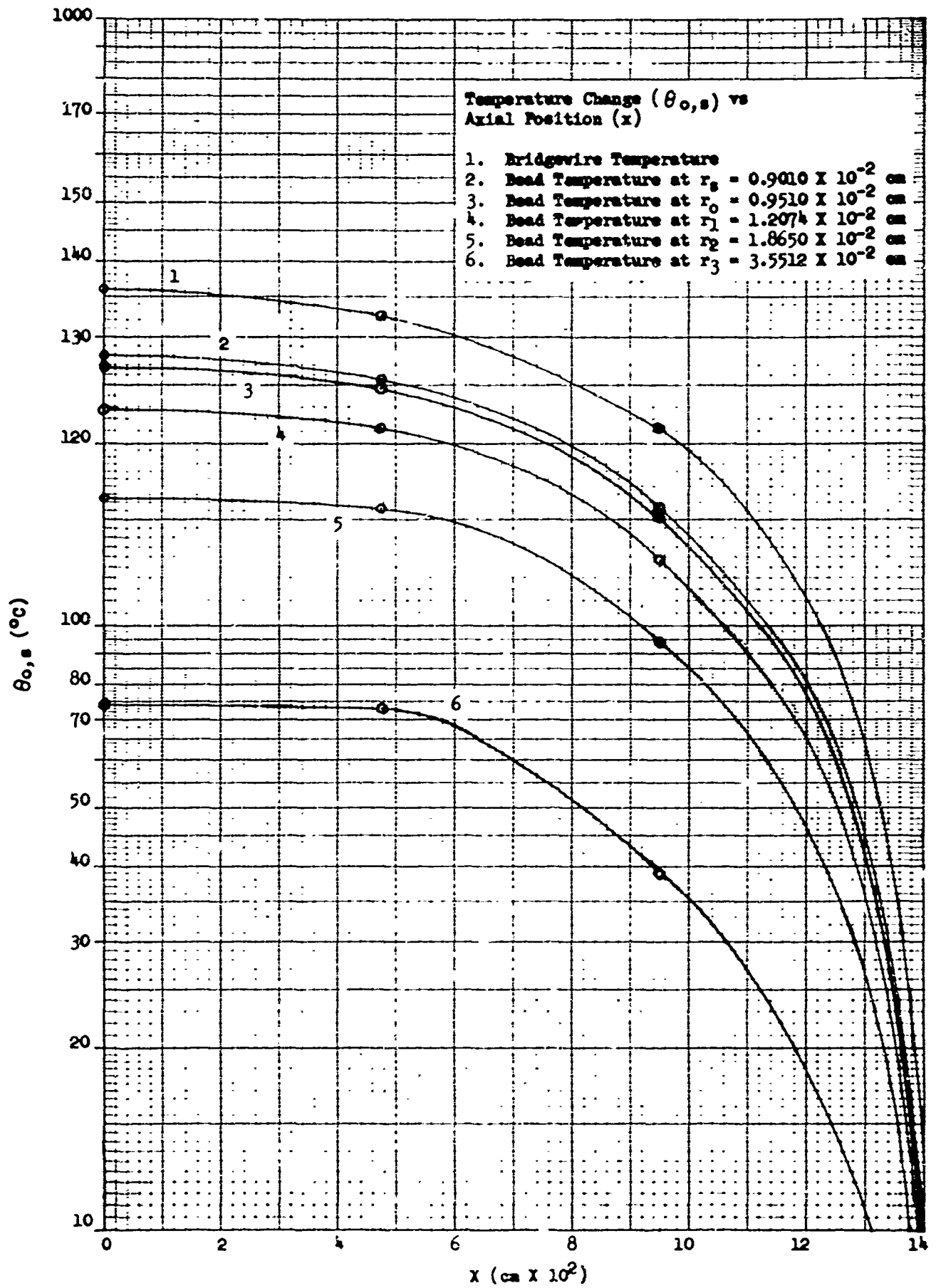


FIGURE 9

STEADY STATE AXIAL TEMPERATURE DISTRIBUTION - I=3 AMPS

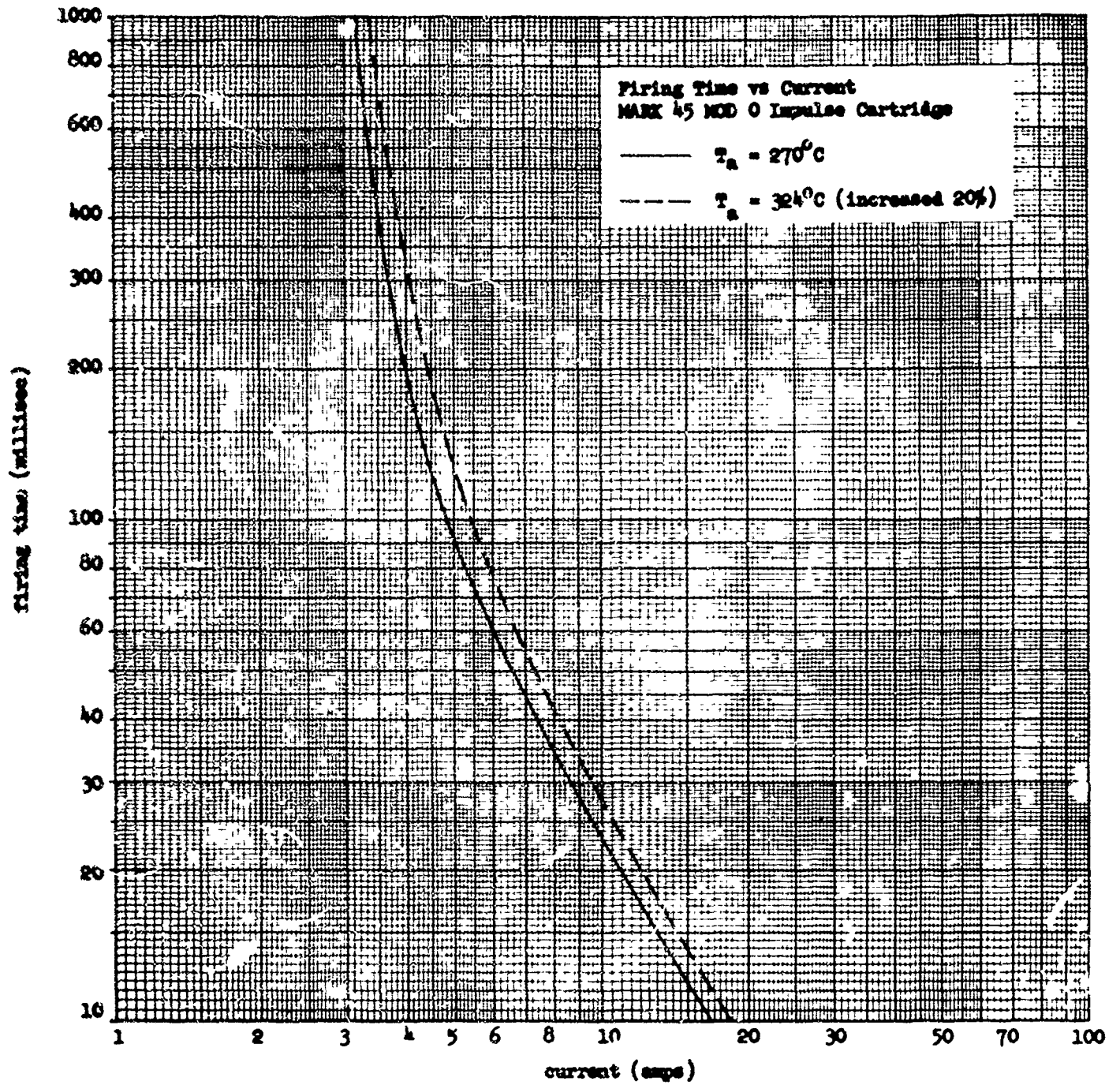


FIGURE 10

EFFECT ON SENSITIVITY OF A 20% INCREASE IN  $T_a$

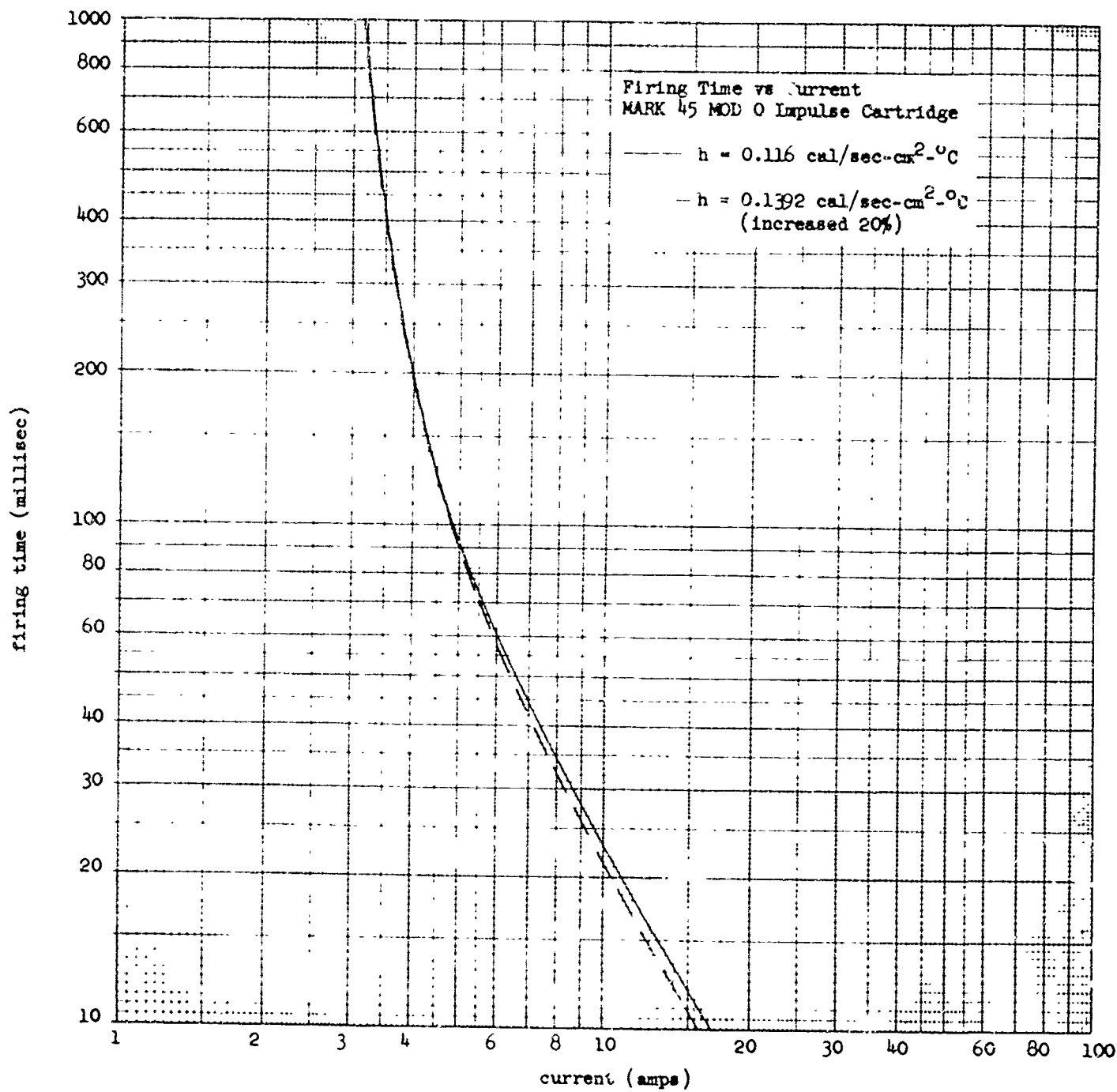


FIGURE 11

EFFECT ON SENSITIVITY OF A 20% INCREASE IN  $h$

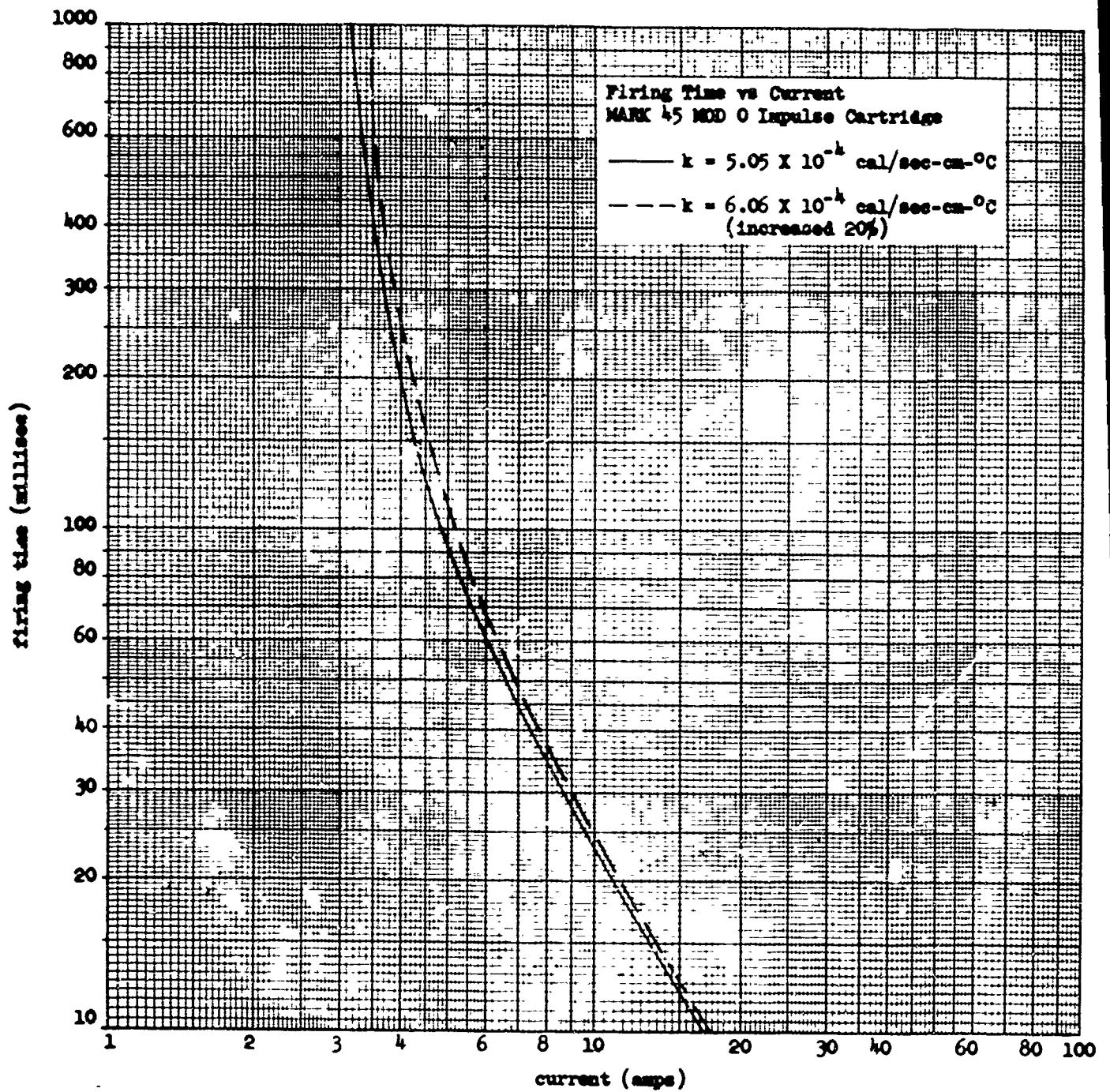


FIGURE 12

EFFECT ON SENSITIVITY OF A 20% INCREASE IN  $k$

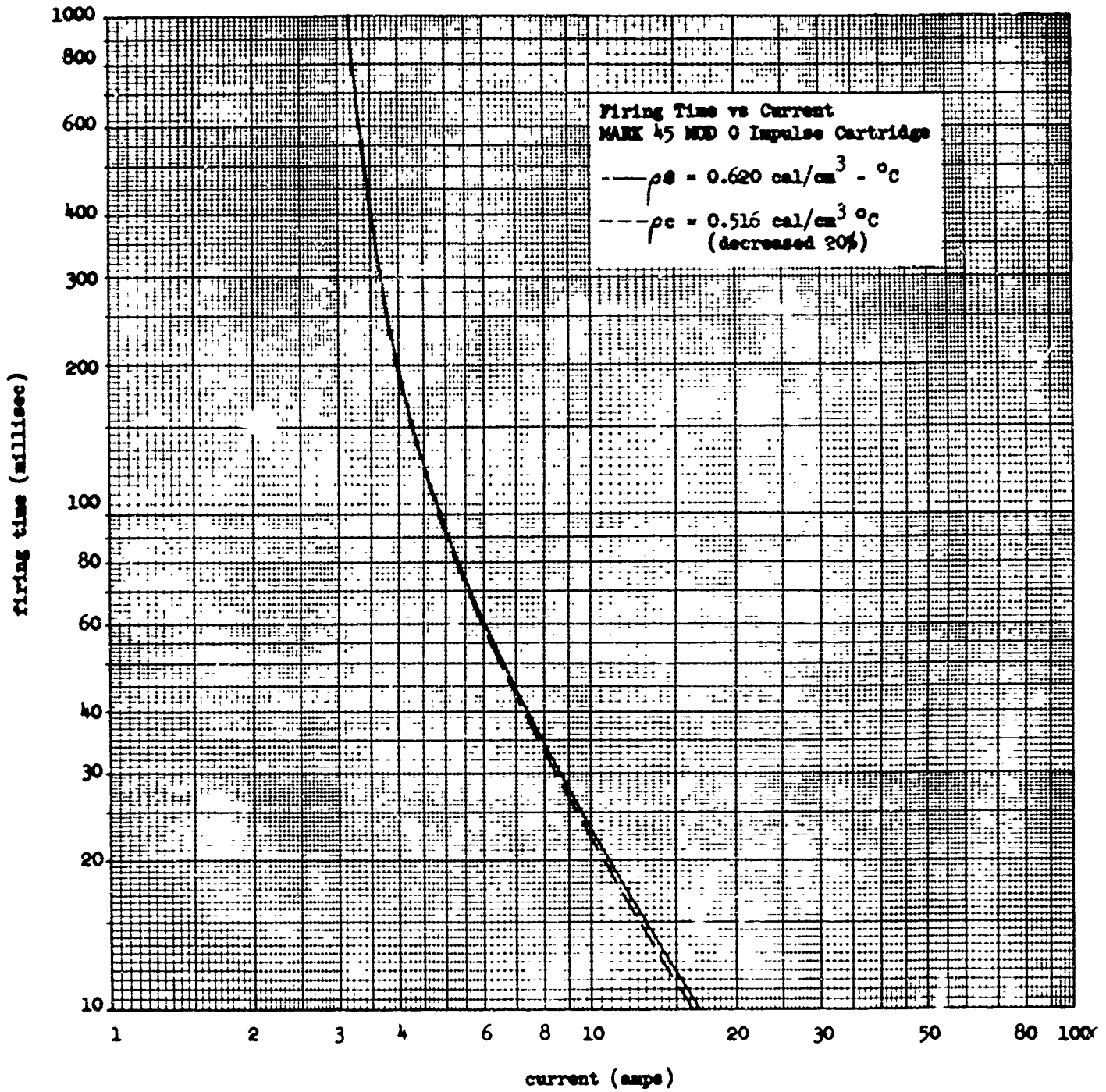


FIGURE 13

EFFECT ON SENSITIVITY OF A 20% DECREASE IN  $\rho_e$

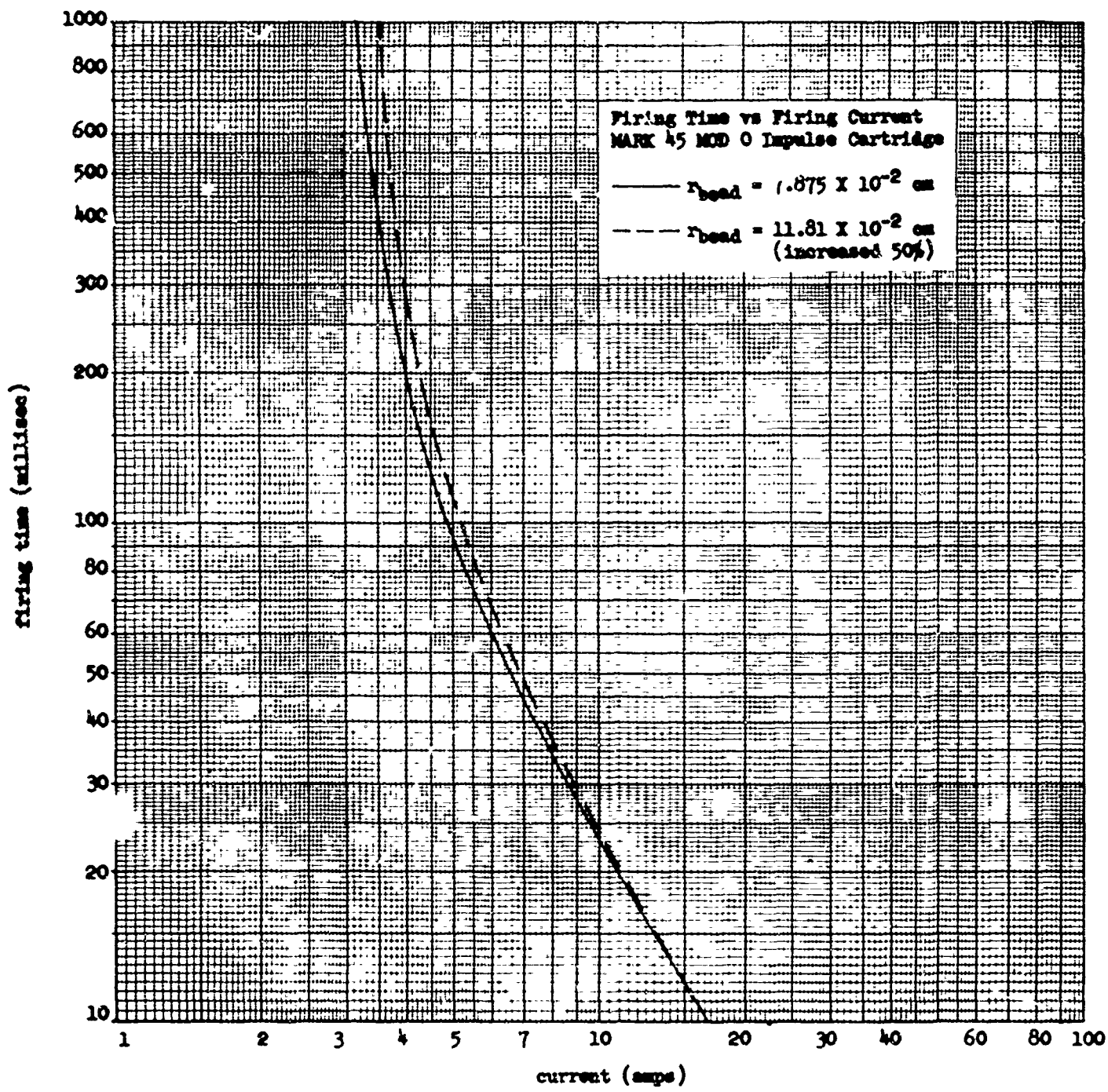


FIGURE 14

EFFECT ON SENSITIVITY OF A 50% INCREASE IN  $r_{bead}$

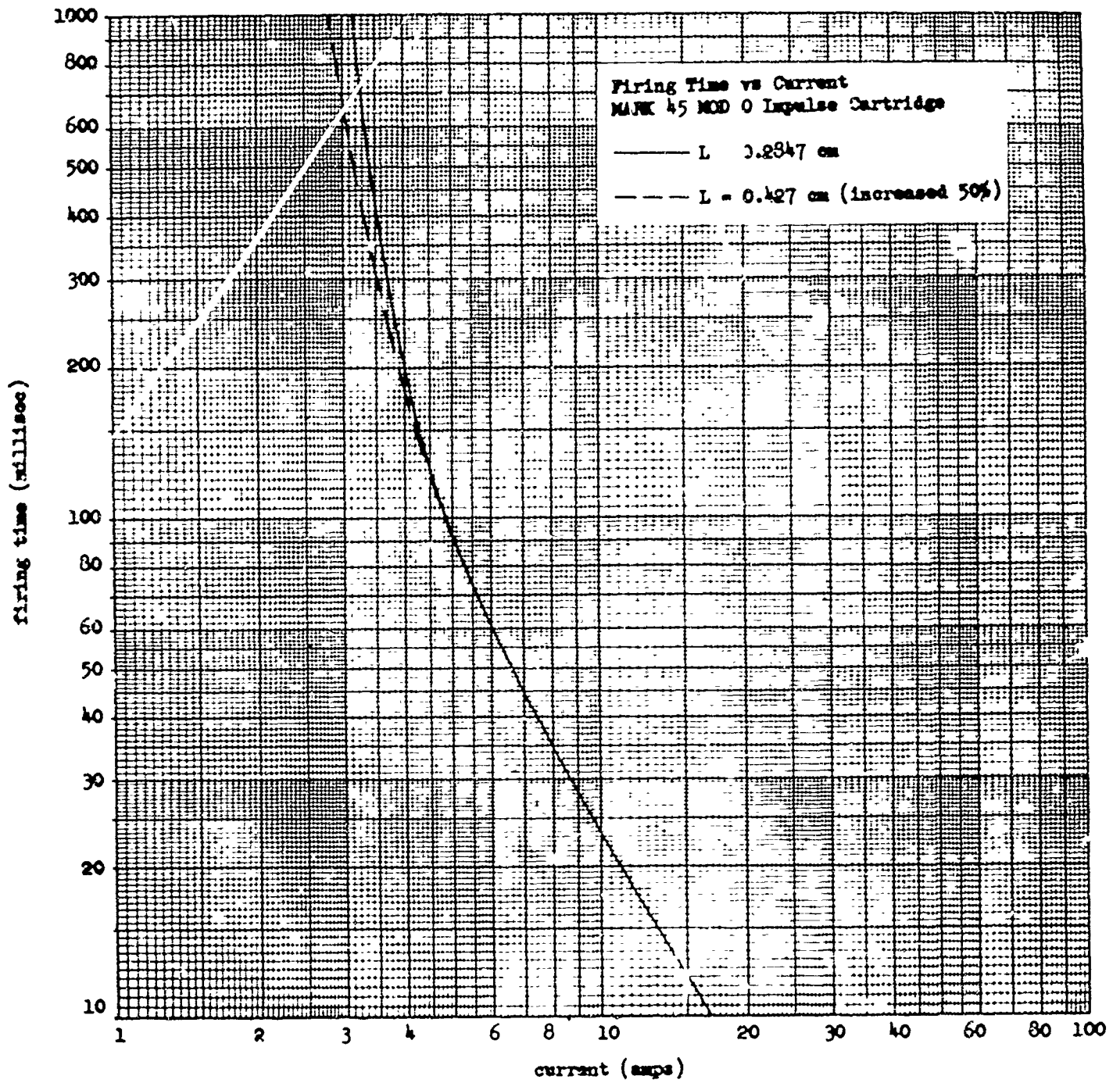


FIGURE 15

EFFECT OF SENSITIVITY OF A 50% INCREASE IN L

The usefulness of the model as a starting point for the design of new hot wire initiators is yet to be demonstrated. However, the work reported here indicates the model is adequate to predict representative firing times versus input stimuli of conventional hot wire initiators.

#### REFERENCES

- (a) Carslaw, H. S. and Jaeger, J. C., Conduction of Heat in Solids, Oxford University Press, Amen House, London E.C.4, 1959
- (b) Cook, M. A., The Science of High Explosives, Reinhold Publishing Corporation, New York, New York, 1958
- (c) Zinn, John and Mader, Charles L., Journal of Applied Physics 31, 323 (1960)
- (d) BUWEPS LD 537926 and all drawings listed thereon - "Cartridge, Impulse, MARK 45 MOD 0"
- (e) Handbook of Chemistry and Physics, 37th edition, 1955
- (f) Fine, Morris E., "Correlation Between Electrical and Thermal Conductivity in Nickel and Nickel Alloys", Journal of Metals 2, 951 (1950)

**APPENDIX A**

APPROXIMATION OF FIRST AND SECOND PARTIAL DERIVATIVES AND THE LAPLACIAN  
BY FINITE DIFFERENCES - UNEQUAL SEGMENTS AND CYLINDRICAL SYMMETRY

The Laplacian in cylindrical coordinates for a system having cylindrical symmetry is

$$\nabla^2 \theta = \frac{\partial^2 \theta}{\partial r^2} + \frac{1}{r} \frac{\partial \theta}{\partial r} + \frac{\partial^2 \theta}{\partial x^2}. \quad (A1)$$

To evaluate  $\frac{\partial^2 \theta}{\partial r^2}$  and  $\frac{\partial \theta}{\partial r}$ , a parabola lying in the  $r$ - $\theta$  plane with  $x=x_n$  is fitted through the three points  $(-p_m, \theta_{n,m-1})$ ,  $(0, \theta_{n,m})$ , and  $(\gamma p_m, \theta_{n,m+1})$  as shown in Figure 16. The equation of this parabola with origin of the coordinate system arbitrarily chosen at radial station  $r=r_m$  is

$$\theta \Big|_{x=x_n} = A(r-r_m)^2 + B(r-r_m) + C, \quad (A2)$$

$$\left. \frac{\partial \theta}{\partial r} \right|_{\substack{x=x_n \\ r=r_m}} = B, \quad (A3)$$

$$\left. \frac{\partial^2 \theta}{\partial r^2} \right|_{\substack{x=x_n \\ r=r_m}} = 2A. \quad (A4)$$

Also,

$$\theta_{n,m-1} = A(-p_m)^2 + B(-p_m) + C, \quad (A5)$$

$$\theta_{n,m} = A(0)^2 + B(0) + C, \quad (A6)$$

and

$$\theta_{n,m+1} = A(\gamma p_m)^2 + B(\gamma p_m) + C. \quad (A7)$$

Simultaneous solution of equations (A5), (A6), and (A7) for A, B, and C yields

$$A = \frac{1}{p_m^2 \gamma(\gamma+1)} \left[ \theta_{n,m+1} - (\gamma+1) \theta_{n,m} + \gamma \theta_{n,m-1} \right], \quad (A8)$$

$$B = \frac{1}{p_m \gamma(\gamma+1)} \left[ \theta_{n,m+1} - (1-\gamma^2) \theta_{n,m} - \gamma^2 \theta_{n,m-1} \right], \quad (A9)$$

$$C = \theta_{n,m}. \quad (A10)$$

Combining equations (A8) and (A9) with equations (A3) and (A4) results in

$$\left. \frac{\partial \theta}{\partial r} \right|_{\substack{x=x_n \\ r=r_m}} = \frac{1}{\gamma(\gamma+1) p_m} \left[ \theta_{n,m+1} - (1-\gamma^2) \theta_{n,m} - \gamma^2 \theta_{n,m-1} \right], \quad (A11)$$

$$\left. \frac{\partial^2 \theta}{\partial r^2} \right|_{\substack{x=x_n \\ r=r_m}} = \frac{2}{\gamma(\gamma+1) p_m^2} \left[ \theta_{n,m+1} - (1+\gamma) \theta_{n,m} + \gamma^2 \theta_{n,m-1} \right]. \quad (A12)$$

To evaluate  $\frac{\partial^2 \theta}{\partial x^2}$  a parabola lying in the  $x, \theta$  plane with  $r=r_m$  is fitted through the three points  $(-q_n, \theta_{n-1,m})$ ,  $(0, \theta_{n,m})$  and  $(\beta q_n, \theta_{n+1,m})$  as shown in Figure 16. Analogous to the approximation obtained for

$\frac{\partial^2 \theta}{\partial r^2}$ , a similar approximation for  $\frac{\partial^2 \theta}{\partial x^2}$  is

$$\left. \frac{\partial^2 \theta}{\partial x^2} \right|_{\substack{x=x_n \\ r=r_m}} = \frac{2}{\beta(1+\beta) q_n^2} \left[ \theta_{n+1,m} - (1+\beta) \theta_{n,m} + \beta \theta_{n-1,m} \right]. \quad (A13)$$

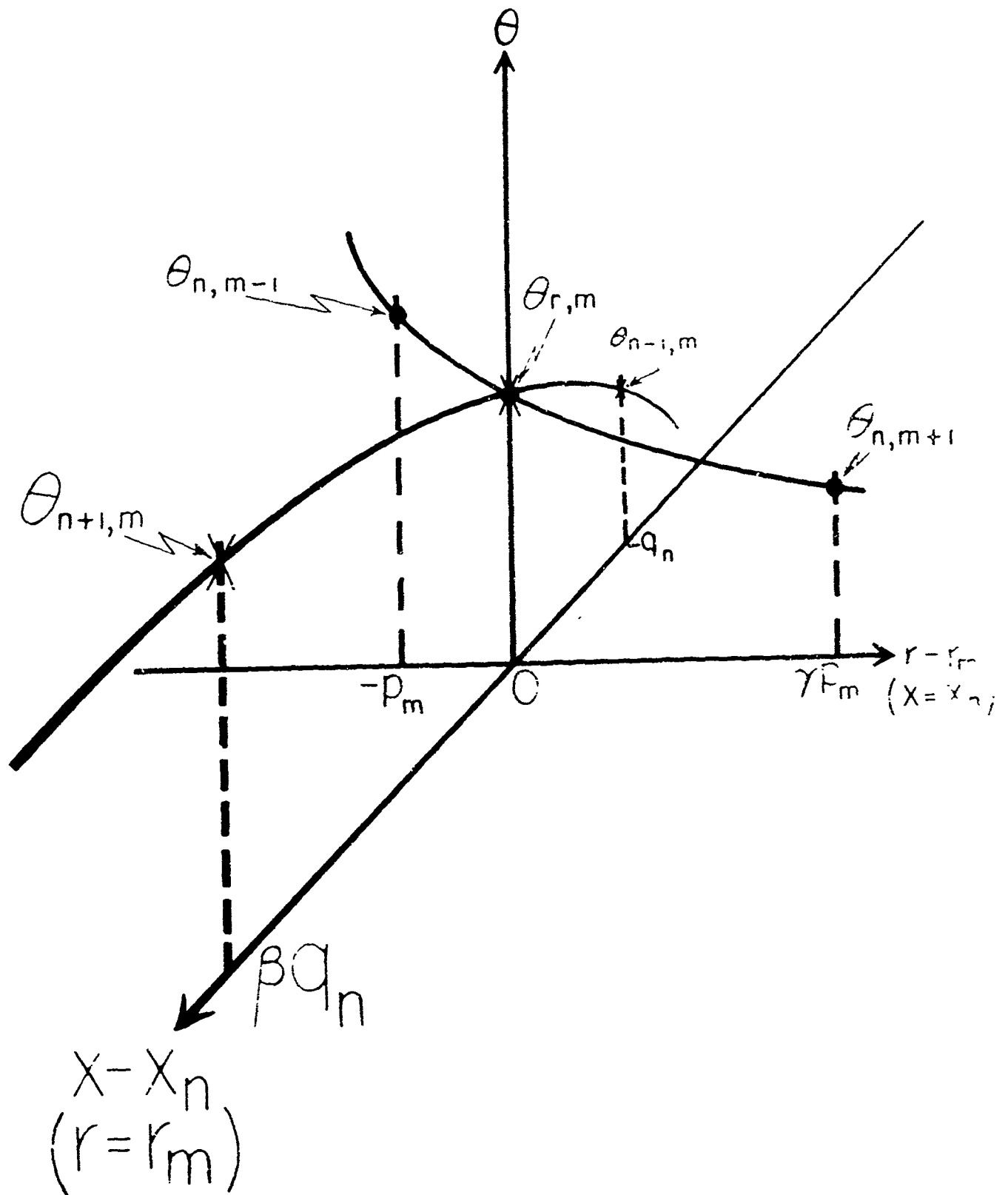


FIGURE 16

FINITE DIFFERENCE CONSTRUCTION FOR  $\frac{\partial^2 \theta}{\partial r^2}$ ,  $\frac{\partial \theta}{\partial r}$ ,  $\frac{\partial^2 \theta}{\partial X^2}$ , AND  $\nabla^2 \theta$

Combining equations (A11), (A12), and (A13) with equation (A1) results in

$$\left. \begin{aligned}
 \nabla^2 \theta \Big|_{\substack{x=x_n \\ r=r_m}} &= \left( \frac{2r_m + p_m}{\gamma(\gamma+1) p_m^2 r_m} \right) \theta_{n,m+1}, \\
 &- \left( \frac{2r_m + (1-\gamma) p_m}{\gamma p_m^2 r_m} + \frac{2}{\beta q_n^2} \right) \theta_{n,m}, \\
 &+ \left( \frac{2r_m - \gamma p_m}{(1+\gamma) p_m^2} \right) \theta_{n,m-1} + \left( \frac{2}{\beta(1+\beta) q_n^2} \right) \theta_{n+1,m}, \\
 &+ \left( \frac{2}{(1+\beta) q_r^2} \right) \theta_{n-1,m}.
 \end{aligned} \right\} \quad (A14)$$

**APPENDIX B**